Robotica (2011) volume 29, pp. 767–785. © Cambridge University Press 2010
doi:10.1017/S0263574710000706

Safe *physical* human–robot interaction of mobility assistance robots: evaluation index and control

Aslam Pervez†,* and Jeha Ryu‡

†*Informatics Complex, P.O. Box 2191, H-8, Islamabad, Pakistan*
‡*Human-Machine-Computer Interface Lab, Department of Mechatronics, Gwangju Institute of Science and Technology (GIST), Gwangju, Republic of Korea. E-mail: ryu@gist.ac.kr*

(Received in Final Form: October 28, 2010. First published online: December 2, 2010)

SUMMARY

Independent mobility is one of the major challenges for elderly. Assistive robots must guarantee user's safety. Existing methods to quantitatively express user's safety are not applicable to mobility assistance robots due to *physical attachment*. This paper proposes a danger index to estimate user's safety during mobility assistance. The formulation and validation of the index is achieved through extensive subjective and objective experimentation. A motion control method is also introduced that uses the proposed danger index for monitoring user's safety and initiating proper safety actions in case of danger. As an example, experimental results with SpiderBot-II are reported in this paper.

KEYWORDS: Danger index; Physical human–robot interaction; Mobility assistance; Elderly.

1. Introduction

The elderly population is increasing in many developed countries. For example, by 2030, the ratio of population above 65 years of age is expected to be 19.6% in the United States, 24.6% in Europe, 31.8% in Japan and 24.3% in Korea.[1] Due to aging and reduced exercises, they feel difficulties in performing activities of daily life (ADLs), such as walking, fetching-and-carrying objects and sometimes even in sitting and standing.[2] Conventional assistive devices (canes and walkers etc.) do not comply with the varying grades of disabilities among elderly.[3] Robotics technology has the potential to provide flexible assistive systems to enable them independent living, provided the user's *safety* is guaranteed. The safety requirement implies that the robot should not harm the user in any situation.[4]

The assistive robots can be identified as *manipulation* (Fig. 1(a)) (for fetch-and-carry-type tasks) and *mobility* (Fig. 1(b)) (for assistance in moving *user's body*, such as walking, lie-to-sit and sit-to-stand etc). Bichhi *et al.* (2008)[5] classified the assistive robots into *hands-on* and *hand-off* types on the basis of *purposeful* physical contact of an *operator's hands* with the robot. Note that in the hands-on assistance, operator is always an active partner guiding the robot, whereas in mobility assistance, a user can be a passive partner.

From Fig. 1 it is clear that mobility (as well as hands-on) assistance robots are different from manipulation assistance robots due to continuous physical interaction between robot and user's body (e.g. hands) during the task. In manipulation (or hands-off) assistance, the physical interaction between robot and the user is only during *accidental* conditions. We shall refer the former continuous physical contact between robot and the user as physical attachment throughout this paper.

Due to physical attachment, the previous safety indices (such as *Gadd Severity Index* (GSI),[8] *Head Injury Criterion* (HIC),[9] *safe impact potential* by Heinzmann and Zelinsky (2003)[4] and a *generalised danger index* by Ikuta *et al.* (2003)[10]) and safety strategies,[11–26] basically developed for manipulation assistance robots, are not applicable to mobility assistance robots (such as wheeled walkers (Care-O-bot,[6] Smart walkers,[27] Walking helper,[28] RT-Walker[30] and PAMAID[31]), installed-walkers (Rail-based arm[3] and SpiderBot-II[20]), sit-to-stand assistance robot (e.g. *gravity-balanced assistive device*[32]) and rehabilitation robot (e.g. *KineAssist*[33])).

As an example, a situation involving an assistive robot moving away from a user is safer in hands-off manipulation assistance scenarios. However, such a situation during walking assistance would pull/push the user and lead to a falling accident. Similarly, an obstacle in the robot path is not a *fundamental* source of danger for a user in the former, whereas it may be a source of danger in the latter. This necessitates the formulation of new indices to assess the safety for users of mobility assistance robots. Interested readers are referred to Pervez and Ryu (2008)[34] for a more detailed review of previous work on safety assessment methods and safety strategies of human-care robots.

This paper proposes the first ever danger index for estimating the threat potentials to the safety of the robot's users during *mobility assistance* scenarios. The methodology adopted to formulate the proposed danger index includes the following: (1) Finding the factors that affect the safety of user, (2) determining the most significant factors through subjective experiments, (3) formulating a simple expression for the danger index relating the most significant factors and (4) validating the expression by correlating the subjective

* Corresponding author. E-mails: aslam@iccc.org.pk, aslam_pervez@hotmail.com

https://doi.org/10.1017/S0263574710000706 Published online by Cambridge University Press

(a) Care-O-Bot[6] © Autonomous Robot 2004 (b) HLPR Chair (NIST)[7] © IEEE 2007



Fig. 1. Assistance scenarios. (a) manipulation (hands-off), and (b) mobility (body attachment).

and objective experiments data through statistical methods (*t*-test for correlation).

The proposed danger index is the weighted *sum* of danger estimates due to *velocity-mismatch* (VMM) between user and robot, and the *distance-to-obstacle*: the two most significant factors that were determined through statistical analysis of the data obtained by subjective experiments. This danger index is different from the one proposed by Ikuta *et al.* (2003)[10] that was defined in terms of distance-to-user, approach velocity towards user and effective inertia of the robot. Note that these factors are not relevant for mobility assistance case because the user is already in physical contact with the robot. The proposed index is validated through extensive experimentation with subjects in mimicked disability conditions during different mobility assistance scenarios using SpiderBot-II.

Furthermore, this paper introduces a motion control method that takes into account the proposed danger index and then applies appropriate safety actions, if necessary, depending on the nature of danger, i.e. varying the velocity of assistive robot in case of VMM, and re-planning a new path for obstacles coming in its way. This method is different from artificial potential field approach[35] because it also takes care of VMM in addition to the distance-to-obstacle. The proposed motion control method is implemented on SpiderBot-II[36] and experimental results are reported in the paper that show an example of practical usefulness of the proposed danger index in realising safe physical human–robot interaction during mobility assistance tasks.

The generality of the proposed index is established through experiments in different mobility assistance scenarios, including walking, lie-to-sit and sit-to-stand. Although we performed the experiments with SpiderBot-II, the proposed danger index is also applicable to other mobility assistance robot systems as well, such as mobile platform-based wheeled walkers (e.g. Walking helper[28] and RT-Walker[30]) and installed walkers (e.g. rail-based arm[3]) etc. This is justified by the fact that the proposed danger index is based on physical variables (VMM and distance-to-obstacle.) that are also detectable (through suitable sensors) in those systems. Moreover, the operational space characteristics of these robots are similar to that of SpiderBot-II, so the experimental results with the SpiderBot-II are also valid for them.

2. Formulation of Danger Index

The major risk for elderly and handicapped during ADLs is the falling accidents because of different reasons. In this work we have only focused on the cases relevant to mobility assistance robots. In order to formulate the danger index, first we considered the situations that can cause a falling accident during mobility assistance and deduced the basic factors leading to those situations. As too many factors may result into a complex expression, we tried to find out a smaller set of the most significant factors through subjective tests. An expression was then proposed to relate the most significant basic factors that got validated by comparing the subjective and objective data through *t*-test for correlation. In the following, we shall discuss each step.

2.1. Factors affecting user's safety

So far, very few robots (for example PAMM-Aid[37]) are evaluated through proper clinical tests and thus the *clinically* proved factors affecting the users' safety are not available. However, from the review of designs and operational modes of different mobility assistance robots, reported in the literature,[6,27–31,33,37–40] certain potentially unsafe situations were pointed out. Guidelines used for selecting the unsafe situations and factors affecting the safety are as follows:

1. Falling accident is the major cause of injuries among elderly.[41]
2. Assistive robots are primarily designed for elderly and handicapped persons.
3. Any situation leading to a potential falling accident must be identified. These situations can be categorised as motion-related or environment-related.
4. In motion-related dangerous situations, the motion variables affecting the physical attachment are selected.
5. In environment-related dangerous situations, the objects (e.g. obstacles) that could initiate a falling accident are identified. As user and robot are physically attached, a collision of robot with any obstacle can break the physical attachment and cause a falling accident or press against obstacle.
6. Owing to a loose physical attachment, small variations in motion variables are absorbed.

https://doi.org/10.1017/S0263574710000706 Published online by Cambridge University Press

Table I. Potentially unsafe situations for elderly.

No.	Situations
1.	Robot moves faster than user.
2.	Robot moves slower than user.
3.	Robot is very near to obstacle (pre-collision case).
4.	Robot collides with obstacles (post-collision case).
5.	Robot end-effector has vibrations/jerks (vibrations and jerks case).
6.	Robot does not follow the desired path (motion inaccuracy case).
7.	Robot task-execution speed is different from user's expectations (task execution).
8.	Robot (e.g. passive walker) needs human power to push (load-to-push case).
9.	Robot is in manual control for a long time (manual control case).
10.	Robot does not support user's weight during walking assistance.

Table I shows a few such situations that can lead to a falling accident during mobility assistance (e.g. walking, sit-to-stand, lie-to-sit, rehabilitation exercise and guidance).

Situations 1 and 2 can be grouped as VMM, whereas situations 6 and 7 can be referred as task performance. As in the case of collision, the impact force is transferred to human body within few milliseconds (typically $\approx$15 ms),[24] post-collision case (situation 4) is of no use for pre-collision safety assessment. In the following subsections, we shall consider each situation in a bit detail and deduce the basic factors. Note that situation 10 is related to the *design* of wheeled-walkers only, and therefore, it is not considered as a basic factor for the formulation of the danger index for general mobility assistance robots.

2.1.1. Velocity-mismatch (VMM). By observing the human–human walking assistance scenarios, it can be easily inferred that for the *safe* assistance there should not be any appreciable VMM between assistive robot and the user. For example, in the walking assistance task, a fast moving robot can push or pull its user, depending on the nature of physical attachment between them, and lead to a falling accident. On the other hand, a slow moving assistive robot may impede the user's movement. Similar comments apply to other mobility assistance scenarios, such as sit-to-stand, lie-to-sit, exercise and guidance. The dynamics of walking assistance is discussed in Appendix A and thereby it is concluded that VMM is very important for safe walking and can be estimated through interaction force variations.

2.1.2. Distance-to-obstacles. The workspace obstacles are the possible sources of collision of robot that can harm the user, who is physically attached with the robot. The distance-to-obstacle can serve as an indicator of the danger for the user in terms of *time to stop the robot before collision* while in motion or the probability of user's collision with that obstacle due to poor posture-balancing capability while not in motion. Note that the collision of robot with obstacle can be more dangerous for a user in mobility assistance scenarios than that in manipulation assistance due to physical attachment.

2.1.3. Vibration/jerks. Vibration and jerks are usually uncomfortable and may be dangerous for some users. However, in many robotic systems, special design methods are adopted such as visco-elastic covering that can absorb the jerks and vibrations. Similarly, a careful trajectory planning (zero jerks, avoiding singularity etc.) could also minimise vibrations and jerks.

2.1.4. Load-to-push. Passive wheeled-walkers (e.g. RT-Walker[30] etc.) require human force to move them and thus they considered as safe device due to absence of powered actuators. However, such passive devices can be a source of physical discomfort for the users. Note that passive robots equipped with servo brakes can exert an additional load of brake torques on their users. In case of *active* wheeled-walkers[29] (equipped with powered actuators) the contribution of this factor will be zero.

2.1.5. Task performance. This involves the accuracy and execution rate etc. of a desired task performed by the assistive robot. If the task execution is too slow and accuracy is not good, it increases the mental discomfort of the user. On the other hand, if the task execution is too fast, it is a source of discomfort and a risk to user's safety.

2.1.6. User's physical and mental condition. The user's physical and mental condition should be used to adjust the safety limits. If the user's physical condition is not suitable, then the safe limits for the above-cited factors that are valid for relatively healthier subjects might be reduced further. The suitable autonomy level of an assistive robot is also dependent on user's physical and mental conditions. In case of stable physical and mental conditions, more authority should be assigned to the user because elderly generally do not like fully autonomous mode of operation.[40]

Among the above-listed factors, the most significant ones affecting the safety of a user during mobility assistance scenarios were found through subjective experiments using the SpiderBot-II.[42] In each experiment, only one factor was varied keeping all others factors constant. After the experiment, subjects were administered questionnaire I (reported in Appendix C.1) about the severity of the factor under test for user's safety. Analysis and results of these experiments are reported in Section 3.7.1.

Even though more rigorous evaluation might be necessary, the preliminary results (reported in Section 3) show that VMM and distance-to-obstacle are the two most significant factors for the *danger* to user's safety.

2.2. Formulation of danger index

Keeping in view the results obtained through subjective tests (reported in Section 3), a scalar function (danger index, D) for estimation of danger potential may be set up as

$$D = \frac{1}{G_h}[w_v D_v + w_d D_d], \tag{1}$$

where G_h = grade of physical health of user ($0 < G_h \leq 1$), w_v = relative weight for VMM-based danger component, w_d = relative weight for distance-to-obstacle-based danger component, D_v = danger due to VMM and D_d = danger due

https://doi.org/10.1017/S0263574710000706 Published online by Cambridge University Press

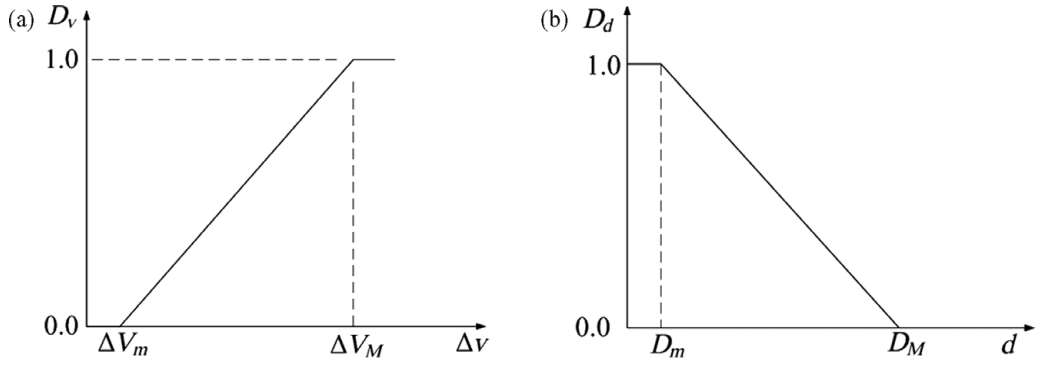


Fig. 2. Graphical representation of (a) D_v (Eq. (2)), and (b) D_d (Eq. (3)).

to distance-to-obstacle (d). D_v and D_d shown in Figs. 2(a) and (b) are given by Eqs. (2) and (3), respectively.

$$D_v = \begin{cases} 0 & \text{if} \quad \Delta v < \Delta V_m \\ \dfrac{\Delta v - \Delta V_m}{\Delta V_M - \Delta V_m} & \text{if} \quad \Delta V_m \le \Delta v \le \Delta V_M, \\ 1 & \text{if} \quad \Delta v > \Delta V_M \end{cases} \tag{2}$$

$$D_d = \begin{cases} 1 & \text{if} \quad d < D_m \\ \dfrac{d - D_M}{D_m - D_M} & \text{if} \quad D_m \le d \le D_M, \\ 0 & \text{if} \quad d > D_M \end{cases} \tag{3}$$

with

$$\Delta v = (\text{sign}\,(\dot{\boldsymbol{x}}_r, \dot{\boldsymbol{x}}_h))\,|\dot{\boldsymbol{x}}_r - \dot{\boldsymbol{x}}_h|, \tag{4}$$

and

$$d = |\boldsymbol{x}_r - \boldsymbol{x}_o|. \tag{5}$$

Here, *sign*(.) is positive for $-\frac{\pi}{2} \le (\angle(\dot{x}_r - \dot{x}_h) - \angle\dot{x}_h) \le \frac{\pi}{2}$ in motion plane (plane defined by $\dot{\boldsymbol{x}}_r$ and $\dot{\boldsymbol{x}}_h$), $\dot{\boldsymbol{x}}_r$ = velocity of robot, $\dot{\boldsymbol{x}}_h$ = human user's velocity, ΔV_M = maximum VMM, above which $D_v = 1$, ΔV_m = minimum VMM, below which $D_v = 0$, $\boldsymbol{x}_r$ = position of robot, $\boldsymbol{x}_o$ = position of obstacle, D_m = minimum distance between robot and obstacle for which $D_d = 1$, D_M = maximum distance to obstacle, beyond which $D_d = 0$. The reference frame of robot is attached at the geometric centre of the SpiderBot-II end-effector, whereas reference frame for human user coincide with standard body coordinate system. Note that Δv is a scalar measure of the VMM given by Eq. (4). It is positive if assistive robot is pulling/pushing the user to comply with robot velocity and negative if retarding the user's self-motion.

Note that unlike the danger index for hands-off manipulation assistance developed by Ikuta *et al.* (2003),[10] D_d does not include the approach velocity because in the mobility assistance we are concerned with elderly and handicapped people (guideline 2, Section 2.1), who in general have poor posture-balancing capability. Thus, an elderly supported by a stationary robot may become unstable and fall on/collide with an obstacle nearby and get injured. Note that elderly need a large base of support (BOS) to compensate for postural sway.[43] Considering only the distance-to-obstacle as a danger measure is though more conservative but safer for the elderly.

Table II. Proposed sensors for danger estimation.

Danger factor/variable	Proposed sensor/method
Velocity-mismatch	Accelerometers[44]/link forces/ vision sensors[45]
Distance-to-obstacle	Vision sensors/ultrasonic range sensors
User's physical health grade	Physical activity scale of elderly (PASE)[41]

Relative weights w_d and w_v show the significance of either factor for the danger to user's safety and can be set by considering the specific user's physical condition. For example, an individual with a leg disability or a stroke survivor cannot walk very fast and thus can be affected by VMM. In this case, w_v should be higher than w_d. On the other hand, for an elderly with weak posture (WP)-balancing capability or with weak eyesight, obstacles can be more dangerous and thus w_d should be higher than w_v.

The proper adjustment of different weights is to be performed through initial assessment with a specific user. Velocity-mismatch and distance-to-obstacle (d) can be estimated online in many ways, as suggested in Section 2.3. The other factors, such as ΔV_M, ΔV_m, D_m and D_M, are the pre-defined constants that can be easily set through simple experimentation for user's walking speed and posture-balancing capability.[42]

It is to be noted that the terms D_v and D_d represent two dimensionless estimates of danger for the elderly; one due to VMM and the other due to distance-to-obstacle. These can be combined in different ways, such as weighted sum or an ordered pair etc. In this work we take their weighted sum for computation of the overall danger index to get an overall estimate because these are basically the two simultaneous components of danger.

2.3. Danger sensing

The reliable sensing of the basic factors comprising the danger index is very important for more precise safety assessment. Table II shows few sensing methods suggested for measuring the basic physical variables of the danger index (D). Velocity-mismatch can be estimated through accelerometers method[44] (in the case of wheeled-walkers), variations in link forces (in the case of installed-walkers) (Appendix A.2) or by vision sensors.[45] Note that independent

https://doi.org/10.1017/S0263574710000706 Published online by Cambridge University Press

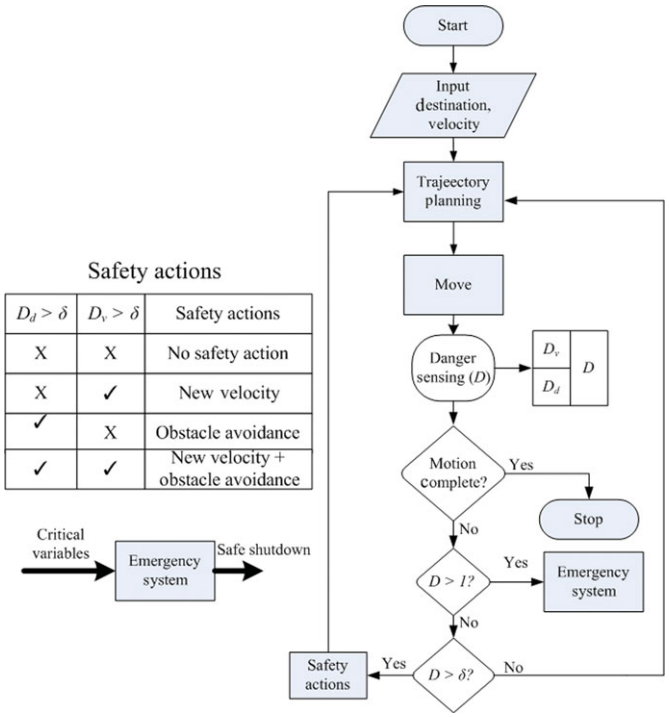


Fig. 3. Flow chart of motion control method for safe physical interaction control.

measurement of human and robot velocities is possible through vision sensors.[45] Once both the velocities are known, VMM ($\dot{\boldsymbol{x}}_r - \dot{\boldsymbol{x}}_h$) can be easily computed.

The distance to the nearest obstacle in unstructured environment can be measured by ultrasonic sensors or vision sensors. User's physical condition can be graded by using Physical Activity Scale for Elderly[41] (PASE), which is a well-established and validated technique to rate the physical activity level of elderly. In this technique, a questionnaire is administered to elderly and based on his activities during last seven days, a score is obtained. PASE addresses the leisure time and household and work-related activities. Questionnaire is available at www.cs.nsw.gov.au/balmain/Strong/Questionnairee/CSM_PASE.pdf. In this method, the time involved in activities are multiplied by the relevant PASE weights to get a numerical value called the PASE score. It has been reported that PASE is positively correlated with grip strength, static balance and leg strength. Thus, the PASE score gives a good estimate about the physical health of a user under trial.

2.4. Safe motion control

Figure 3 shows a motion control method for the safe *physical* human–robot interaction control of mobility assistance systems. This method takes into account the proposed danger index and determines the proper safety action during the task. Note that our aim by introducing this method is to show an example of the practical use of the proposed danger index for initiating a proper safety action. In this figure, the *trajectory planning* block converts the desired destinations (X^d) specified in Cartesian space into joint space for nominal moving velocity (V_n). During the movement, the danger index is continuously updated through Eq. (1).

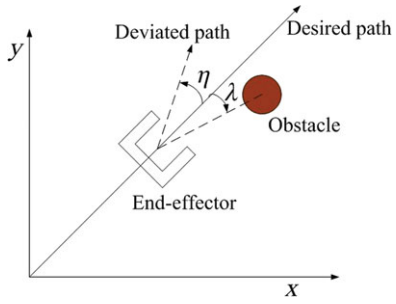


Fig. 4. Obstacle avoidance strategy.

A danger index greater than unity indicates that the safety of user is severely threatened. For such a situation persisting for a threshold time limit, emergency system is called in to shutdown the robot safely. If the danger index is within a threshold (δ), the command motion is carried out without any modification. For a danger index (D) between unity and the danger threshold (δ), appropriate safety action (listed in table at the top-left in Fig. 3) is generated. In case of a danger due to VMM, new reduced velocity, V_n', is calculated as

$$V_n' = V_M - D_v\,(V_M - V_m), \tag{6}$$

where V_M, V_m, are the maximum and minimum moving velocities, respectively, and D_v is the danger due to VMM as defined in Section 2.2. In case, $\|V_n - V_n'\| \leq \Delta_{th}$, then V_n is retained. Here, V_n is the command movement velocity and Δ_{th} is the velocity change threshold.

For the case of danger due to distance-to-obstacle, obstacle avoidance action is initiated. Note that obstacle avoidance is a well-researched area and various techniques are available for it in the literature (e.g. Khatib, 1985[35]). In this work we used a simple method to avoid the nearest obstacle by moving the robot in a deviated direction on the basis of D_d (danger due to distance-to-obstacle) and λ (the angle between the robot-to-obstacle vector and the desired-path). The angle of deviation (η) with respect to the desired path is given by Eq. (7). Angles (η) and (λ) have been defined in Fig. 4

$$\eta = \begin{cases} -D_d \dfrac{\pi}{2} & \text{if} \quad 0 \leq \lambda < \dfrac{\pi}{2} \\ D_d \dfrac{\pi}{2} & \text{if} \quad -\dfrac{\pi}{2} \leq \lambda < 0. \end{cases} \tag{7}$$

While avoiding the obstacle, as the robot moves away from obstacle, D_d reduces and thus the deviation angle η also reduces. When the latter approaches to zero, robot will be on its original desired path.

2.5. Implementation on SpiderBot-II

Figure 5 shows the implementation of motion control method, presented in Section 2.4, on SpiderBot-II (Appendix B) and highlights its main blocks. The trajectory planning block defines the motion trajectory for each axis controller using the desired destination X^d (predefined or input by user depending on the mode of operation (Appendix B)), nominal moving velocity (V_n) and actual pose of an end-effector, X. Nominal velocity, V_n, initially

https://doi.org/10.1017/S0263574710000706 Published online by Cambridge University Press

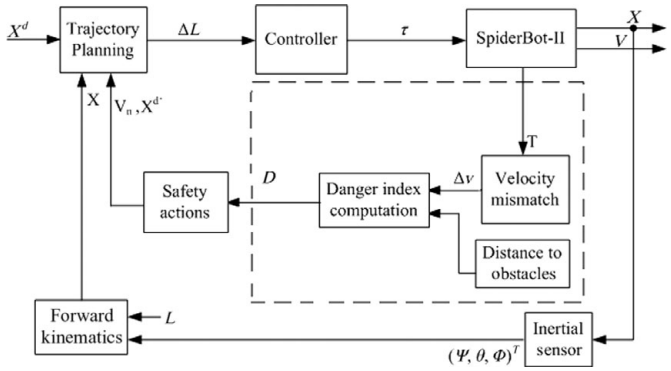


Fig. 5. Block diagram of implementation of motion control algorithm on SpiderBot-II.

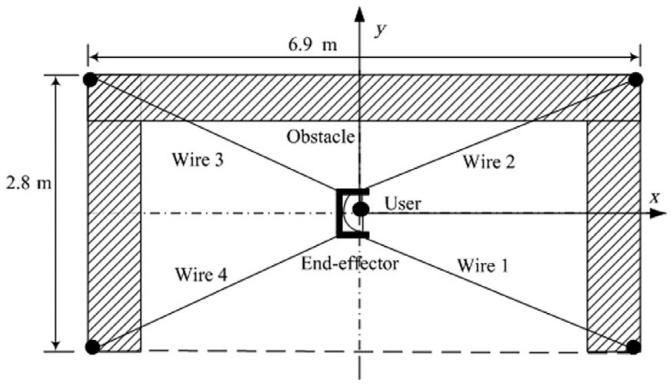


Fig. 7. Top view of experimental environment.

set in accordance with the average walking velocity of user, is used to compute the actuators' velocity for the desired motion trajectory.

During the motion, if the danger index exceeds the threshold, then a new velocity is computed using Eq. (6), as discussed in Section 2.4. Inverse kinematics model (Eqs. (B5 and B6)) is used to compute the wires' length variations ($\boldsymbol{\Delta L} = \boldsymbol{L}^d - \boldsymbol{L}$), where $\boldsymbol{L}^d$ is the vector of wires' length for the desired pose ($\boldsymbol{X}^d$) and $\boldsymbol{L}$ is the vector of wires length at the actual pose ($\boldsymbol{X}$), both determined through inverse kinematics using Eq. (B5). The computed ΔL_i are linearly interpolated and fed to the ith axis controller for driving the actuator.

In this work, VMM was estimated by variations in wires' tension (measured through load cells, SUU-100 K) installed in series with wires (Fig. B1(b)) by using Eq. (A6). The blocks used for computation of the danger index through Eq. (1) are marked by dotted lines in Fig. 5. Computation of VMM by wires' tension is briefly discussed in Appendix A.2. For further details, see ref [39].

3. Experimental Results

In order to find the most significant factors affecting the safety of a user, to validate the proposed danger index and to show its usefulness for safe *physical* human–robot interaction (pHRI) control, we performed extensive experiments with subjects in mimicked disability conditions. Accordingly, three sets of experiments were performed: Set I for finding significant factors affecting user's safety; set II for validating the proposed danger index and set III for showing the effectiveness of the proposed danger index through motion control method given in Section 2.4. SpiderBot-II was used as an experimental platform for this work. In the following, we discuss the design of experiments, major steps and results of these experiments.

3.1. Assistance scenarios

Three mobility assistance scenarios, namely walking (Fig. 6(a)), sit-to-stand (Fig. 6(b)) and lie-to-sit (Fig. 6(c)) were considered for experiments, because these are common ADLs of elderly and disabled. Top view of experimental environment is drawn in Fig. 7 that shows the geometry and available space for conducting experiments.

3.2. Recruitment of subjects

We recruited healthy subjects, who were graduate students and staff, including 17 males and 3 females having 23–43 years of age (mean age: 28.85 years; SD: 5.65 years). These subjects were chosen because of general unavailability/unwillingness of elderly to participate in such experiments.

3.3. Mimicking disabilities

There are so many diverse levels of disabilities or weaknesses among elderly and handicapped that it is very difficult to mimic every case. We considered three disability conditions that are more common among them, namely leg disability,

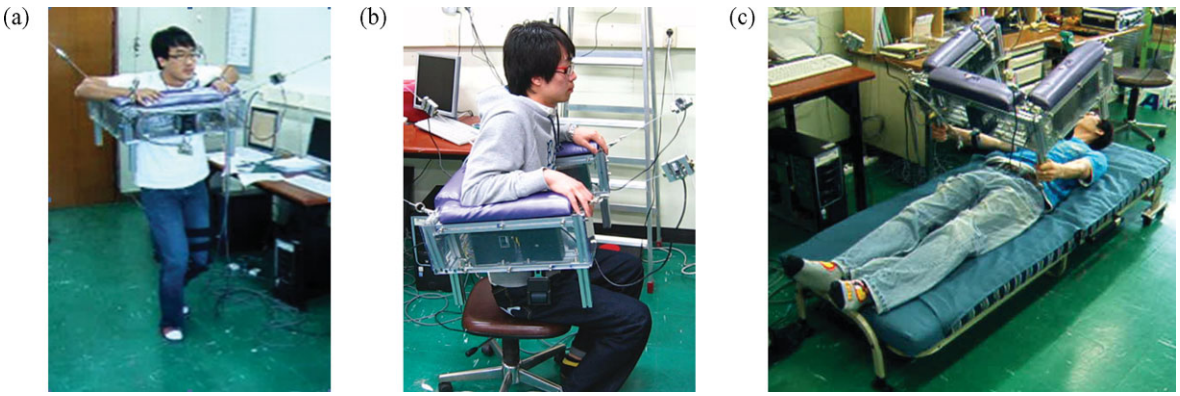


Fig. 6. Assistance scenarios for experiments. (a) walking, (b) sit-to-stand and (c) lie-to-sit.

https://doi.org/10.1017/S0263574710000706 Published online by Cambridge University Press

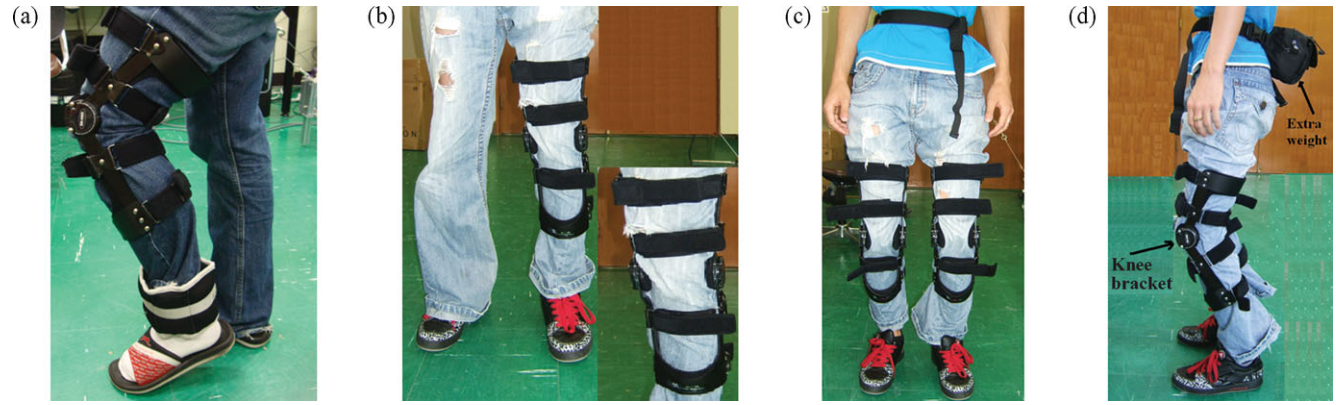


Fig. 8. Mimicking the disability conditions. (a) leg disability, (b) knee disability, (c) weak posture (front view) and (d) weak posture (side view).

knee disability and weak posture balancing. In order to mimic the disability conditions, we used a pair of knee braces and a pair of ankle weights (1.1 kg each) in consultation with Dr. Yang Won-Ho (Head Rehabilitation Hospital, Cheomdon, Gwangju, South Korea). The braces were clamped to subject's leg(s) for fixing the corresponding knee at a desired angle from the available choices (0°, 15°, 30°, 45°, 60°, 75°and 90°). Ankle weights are commercially available sand bags to be worn around legs and are commonly used by athletes for exercise.

The leg disability was mimicked by setting the brace angle at 90°and wearing the ankle weight (1.1 kg), as shown in Fig. 8(a). For mimicking the knee disability (Fig. 8(b)), subject had to wear the knee brace set at 0°in one leg for restricting the knee from bending. The weak posture balancing (Figs. 8(c) and (d)) was mimicked through wearing the ankle weights and knee braces (set at 60°) in both the legs and inserting an additional weight of $2 \sim 4$ kg in the back pouch (Fig. 8(d)). Note that due to the mimicked leg disability subjects were unable to exert any load on that leg, whereas with the mimicked knee disability subjects' knee was restrained from bending. Similarly, a weak posture balancing refers to the condition where a subject was unable to stabilise his body in the standing posture and was susceptible to fall without proper support.

3.4. Design of questionnaire

As no standard questionnaire was available in the literature for the subjective experiments related to physical human–robot interaction, we had to develop the questionnaires for this work. Two questionnaires were prepared, one for screening the most significant factors affecting the user's safety during mobility assistance scenarios and the other for validating the proposed danger index. For this purpose, various test situations were artificially generated during these mobility assistance scenarios and relevant parts of the questionnaires were administered on subjects after each test. Some questions were qualitative with five options (SA: strongly agree, A: agree, U: undecided, D: disagree and SD: strongly disagree), whereas others were quantitative containing Lickert-type scale (ranking $0 \sim 4$ with 4 as the most severe case).

Questionnaire 1 (Appendix C.1) was aimed at investigating the effects of velocity-mismatch (VMM), distance-to-obstacle, vibrations, jerks, motion inaccuracy and load-to-push on the user safety during mobility assistance tasks. The velocity-mismatch refers to the condition in which velocity of robot and human were not harmonious. Questions 1 and 3 (VMM test) were qualitative in nature, whereas questions 2 and 4 were for quantitative analysis. The idea behind questions 2 and 4 was to quantify the pushing/pulling force in reference to a falling accident or retardation to user's movement. *Obstacles-in-the-way* (test 2) refers to a situation in which an obstacle comes in the path while robot is assisting a human user. Similar to VMM part of the questionnaire, question 1 was qualitative, whereas questions 2–3 were for quantitative analysis. The *vibration and jerks* part of the questionnaire was aimed at finding the risk of falling for a user when a robot end-effector exhibits oscillatory behaviour and jerks. In this part, questions 1, 3 and 5 were qualitative, whereas questions 2, 4 and 6 were for quantitative analysis.

The *motion-inaccuracy* part of the questionnaire was to investigate the user's safety when an assistive robot shows an error between command position and actual position. All the questions were quantitative in nature and focused on risks for user's safety. The *load-to-push* part of the questionnaire 1 was to get users' opinion about passive robots that require user's force to push them: Here, question 1 was qualitative, whereas question 2 was for quantitative analysis.

Questionnaire 2 (Appendix C.2) was developed to obtain the subjective data about danger to user's safety during the test situations in mobility assistance tasks. Here, test 1, the VMM case, was to rate the severity of danger due to VMM, whereas test 2, obstacles case, was to rate severity of danger due to obstacle(s) in the robot path during walking assistance task. These tests were repeated with leg disability, knee disability and weak posture-balancing conditions. In both parts, all the questions were for quantitative analysis.

Tests 3 and 4 of the questionnaire were to investigate the VMM effect during sit-to-stand and lie-to-sit assistive tasks. The main assumption was that posture balancing is very important for elderly to avoid falling accident during these tasks. In both tests, questions 1 and 2 were qualitative, whereas question 3 was quantitative in nature.

https://doi.org/10.1017/S0263574710000706 Published online by Cambridge University Press

3.5. Procedure

In set I experiment, the significance of VMM, distance-to-obstacle, jerk, oscillations and motion inaccuracy on the danger to subjects' safety were investigated. For VMM (test 1), SpiderBot-II was used for assisting a subject in mimicked disability condition during walking. The SpiderBot-II end-effector moving velocity (V_n) was varied during the test. Subjects were unable to comply with the variations in velocity due to mimicked disability.

In test 2, distance-to-obstacle, an obstacle was placed in motion path and users were asked to rate the severity of danger to their safety when near and far from the obstacle. A near obstacle means an obstacle at a distance <0.1 m, whereas a far obstacle refers to an obstacle at a distance >1 m. For the oscillation test (test 3), sustained oscillations at different frequencies were generated at the SpiderBot-II end-effector, whereas for the jerk test, a random jerk was created during the assistive tasks (walking, sit-to-stand and lie-to-sit). For the motion inaccuracy test (test 4), robot destination was varied randomly within a radius 0.25 m in motion plane. Command destination was already identified for subjects by putting a mark there. In load-to-push test, subjects' opinions for danger to their safety were sought about the passive robots that need human force to move them.

Random trials of these tests were carried out with different subjects. After each experiment, subjects were administered the relevant part in questionnaire I. All the subjects were interviewed after the experiments to investigate if any subject got frightened. However, none of them was found to have such feeling. It was done to confirm that subjects were pointing out the real danger (damage probability) and not just the danger feelings. The statistical analysis of the subjective data obtained in set I experiments through questionnaire 1 is presented in Section 3.7.1.

Set II of experiments was carried out for validating the proposed danger index (Eq. (1)). In these experiments, VMM, and distance-to-obstacle were considered as test situations. In the VMM test (test 1), users with mimicked disability condition were assisted by the SpiderBot-II end-effector while walking on a straight path. During the test, velocity of the SpiderBot-II end-effector was varied twice at instants unknown to subjects and thus three distinct velocity phases were created. After the test, subjects were asked to describe the severity of danger in each velocity phase.

In the distance-to-obstacle test (test 2), subjects with mimicked disability condition were assisted by the SpiderBot-II end-effector for walking on a straight path. An obstacle was placed in the path of the SpiderBot-II end-effector. Thus two different motion phases were obtained: *obstacle near* (*end-effector* D2O $<$ 0.1 m) and *obstacle far* (D2O $\geq$ 1 m). After the test, subjects were asked to describe the severity of danger in both motion phases. Both tests were repeated for leg disability, knee disability and weak posture-balancing conditions. In the third test, subjects in mimicked weak posture balancing were tried for the VMM case during sit-to-stand task using SpiderBot-II for assisting the subject. During the test, velocity of the SpiderBot-II end-effector was varied and thus distinct velocity phases were available. After the test, subjects were asked to reply the relevant part of the questionnaire 2. Similar procedure was used in the fourth test for lie-to-sit assistance task. The subjective data obtained through questionnaire 2 was then compared with the average values of the danger index computed online during the same test using *t*-test for correlation. The analysis and results of the *t*-test are reported in Section 3.7.2.

3.6. Data collection

Random trials of these tests were carried out with different subjects. Four sets of variables were recorded during the experiments, namely, *desired motion trajectory*, *measured variables*, *computed pose* and *computed signals*. The measured variables included end-effector orientations, wire-lengths, wire-tensions and actuator velocities. The computed pose is the end-effector pose using forward kinematics (Eq. (B7)), whereas the computed signals set included VMM (Eq. (A3)), distance-to-obstacle and danger index (Eq. (1)), computed during the experiment. The distance to the nearest obstacle was computed online since the exact pose of the obstacle was known in the test set-up.

3.7. Statistical analysis and major results

3.7.1. Screening of significant variables. The subjective data collected through set I experiments was used to screen the most significant variables (large influence) affecting the user's safety during mobility assistance tasks by using Principal Component Regression[46] (PCR), a regression model using the principal components as independent variables. Principal components are variables that are mutually independent. The variable influence ρ of principal component (t_i) is given by[46]

$$\rho = \frac{\sum_{i=1}^{p} SSR(t_i)\, p_{ij}^2}{SSR(t_1, t_2, t_3 \ldots t_p)}, \tag{8}$$

where $SSR(t_i)$ is the variance explained by the principal components when a PCR model is developed, $SSR(t_1, t_2, t_3 \ldots t_p)$ is the total variance explained by the principal components and p_{ij} is the loading vector between principal component t_i and independent variables X_j. The Matlab^{TM} function *princomp*(Y) was used to find the loading p_{ij} of data matrix Y; rows of Y correspond to observations and columns to variables X_j.

The results of this analysis are shown in Table III. In this table, the second row gives the influence (ρ) of each variable affecting the user's safety. Thereby, it is evident that VMM and distance-to-obstacle seem to be the two most significant factors contributing to the danger.

3.7.2. Validation of danger index. In order to validate the proposed danger index (Eq. (1)), a *t*-test for correlation was performed on the subjective data collected through questionnaire II and the corresponding objective data comprising the average values of the proposed danger index during the experiment of set III. In this analysis, null hypothesis was that there is no correlation between the subjective and the objective data, i.e.

https://doi.org/10.1017/S0263574710000706 Published online by Cambridge University Press

Table III. Significance of basic variables for danger.

Variables	Velocity-mismatch	Distance-to-obstacle	Vibration	Motion inaccuracy	Load-to-push	Jerks
Danger to safety	5.63	8.83	3.76	4.81	4.68	4.08

Table IV. Results of *t*-test for correlation.

Index	Observations (n)	Correlation coefficient (R)	Computed (T_0)	Critical (T_0)	p-value
Danger	65	0.71	8.10	2.66	<0.005

$$H_0 : \rho = 0 \quad \text{(null hypothesis)},$$
$$H_1 : \rho \neq 0 \quad \text{(alternate hypothesis)}.$$

The appropriate test statistic for these hypotheses is $T_0 = \frac{R\sqrt{n-2}}{\sqrt{1-R^2}}$, which has t-distribution with $n-2$ degrees of freedom if $H_0 : \rho = 0$ is true. Therefore, we will reject the null hypothesis if $|t_0| > t_{\alpha/2n-2}$. Here, $R = \frac{S_{XY}}{[S_{XX}S_{YY}]^{1/2}}$ with $S_{XY} = \sum_{i=1}^{n} Y_i(X_i - \overline{X})$ $S_{XX} = \sum_{i=1}^{n}(X_i - \overline{X})^2$ and $S_{YY} = \sum_{i=1}^{n}(Y_i - \overline{Y})^2$. Here, n is number of observations, X_i and Y_i are the subjective value for danger and the computed value of the proposed danger index during the experiment, respectively.

The results of t-test for correlation are presented in Table IV. The computed values of sample correlation coefficient (R) and T_0 for the proposed danger index are 0.71 and 8.10, respectively. Note that the critical values of T_0 for 60 observations ($\alpha = 0.005$) is 2.66.[47] Therefore, the null hypothesis (i.e. no correlation exists) was rejected at $p < 0.005$. Thereby, it was concluded that a correlation exists between the subjective data and the objective data of the proposed danger index and this validated our proposed danger index.

3.8. Safe motion control

Set III of experiments was aimed at showing the practical usefulness of the proposed danger index in terms of ensuring the safe motion control of an assistive robot through the motion control method (Section 2.6). In this experiment, two cases were considered, namely VMM and obstacle-in-the-way. Results are shown in Figs. 9 and 10.

3.8.1. Case 1: Velocity-mismatch. In the VMM case, the SpiderBot-II was commanded to move in a straight line from (−1.0, 0, 1.32) to (1.2, 0, 1.32) with the nominal linear velocity of 0.4 m/s, assisting a subject in the mimicked weak posture-balancing condition. The motion started at time $t \approx 2$ s and was completed at $t \approx 8$ s (see curve x in Fig. 9(a)). The subject could not follow the robot due to the mimicked disability and thus VMM occurred between them. The tension in the wires 1 and 2 increased (Fig. 9(b)) due to VMM because the robot was pulling the subject. Closer views of wire tension curves at time $t = 2$–4 s and $t = 4$–6 s, associated with increase in VMM, are shown in Figs. 9(c) and (d), respectively.

As discussed in Section 2.4, the safety action in such a situation is to reduce the moving velocity. When the danger index exceeded the threshold value (0.2) at time $t \approx 3$ s (Figs. 9(a) and (e)), a new linear velocity was computed using Eq. (6) and actuators' velocities were modified accordingly, as shown in Fig. 9(f). As a result, both VMM and danger index were reduced. The danger index (D) again increased at time $t \approx 5.25$ s because of VMM, but this time the previous velocity was retained because new linear velocity (computed by Eq. (6)) was less than the *velocity change threshold* (Δv_{th}) from the existing velocity at that time. This threshold was to avoid the frequent variations in the command velocity because it can be uncomfortable for the elderly. Note that in this test, the obstacle did not contribute to the danger index due to obstacle being at large distance from robot (D2O > 2 m).

3.8.2. Case 2: Obstacle. For the *obstacle* case, we set the relative weight of VMM-based danger (w_v) to zero for avoiding the small variations in VMM to be reflected in danger index during this test. The experiment environment was same as shown in Fig. 7; however, an obstacle was considered at (0.8, −0.65, 0.0) in the motion plane. The SpiderBot-II was commanded to move in a straight line from (−1, 0, 0) to (1, 0, 0), as can be seen in Fig. 10(a). The motion was started at time $t \approx 2$ s and was completed at $t \approx 20$ s. During the motion, the distance-to-obstacle was computed online (Fig. 10(b)). Owing to obstacle, the danger index exceeded the threshold ($\delta = 0.2$) at time $t \approx 13$ s and a safety action (obstacle avoidance) was initiated. In the *obstacle avoidance* action, the human–robot compound was moved on a deviated path in order to avoid the collision with the obstacle. This deviation can be observed by initiation of movement in y-direction in Fig. 10(a) at time $t \approx 13$ s. Due to this deviated path, the distance-to-obstacle started to increase and consequently the danger index started to decrease.

Note that command position was not achieved because even after reaching at deviated destination (−1.2, −0.25, 1.32), the danger index was still non-zero (∼0.08). Also note that in this test, VMM was very small because the velocity of the subject was almost same as that of the robot end-effector assisting him during walking.

https://doi.org/10.1017/S0263574710000706 Published online by Cambridge University Press

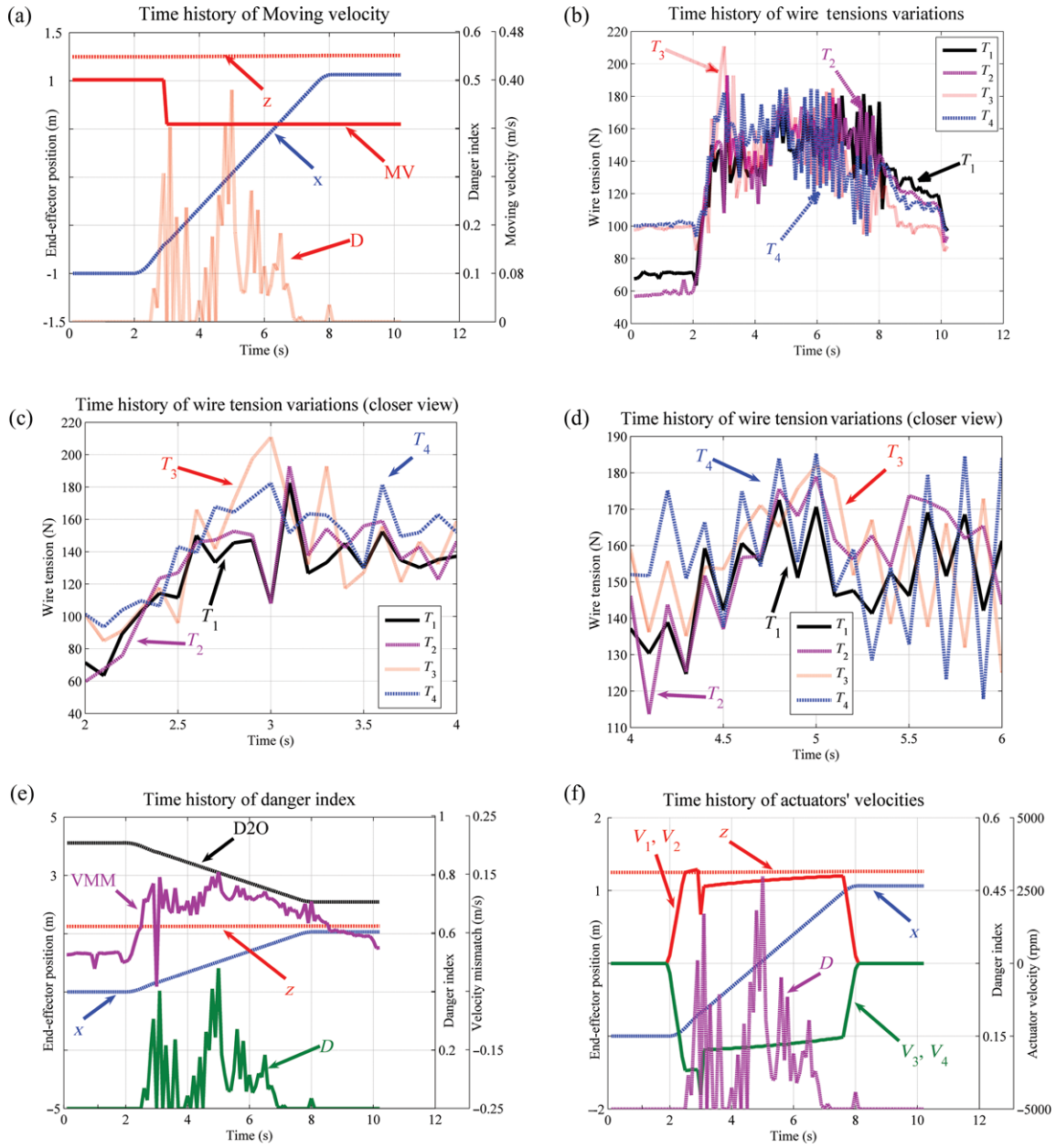


Fig. 9. Experimental results for velocity-mismatch case.

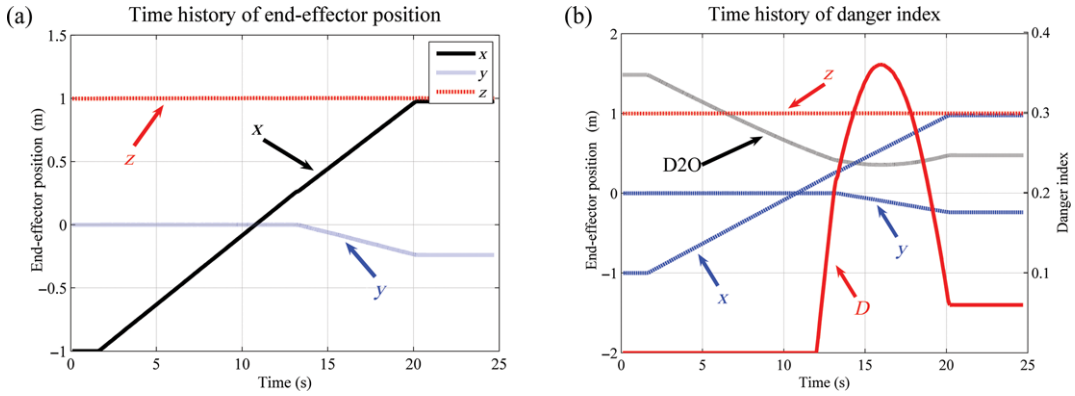


Fig. 10. Experimental results for obstacle case.

https://doi.org/10.1017/S0263574710000706 Published online by Cambridge University Press

3.9. Discussion

This paper proposes the danger index for pointing out the lack of user's safety during mobility assistance scenarios. As this index is related to the safety of human users, we have conducted extensive experiments with different subjects using SpiderBot-II. These experiments were aimed at finding the significant factors that affect the *safety* of a user, validating the proposed danger index, and showing the usefulness of the proposed index for enhancing user's safety. As elderly were not available/willing to participate in such experiments, we used healthy subjects with mimicked disabilities (leg, knee and weak posture balancing). In order to provide an insight to interested readers, these experiments have been briefly described in Appendix D.

The velocity-mismatch was found as one of the most significant factors for the proposed danger index. For estimating VMM we used the wire tensions through load cells installed in series with the wires near the end-effector. However, wire tension signals are noisy, as can be observed in Figs. D1–D8. Other sensors, suggested for VMM in Table II, may be used for obtaining more accurate VMM.

In these experiments, the maximum moving velocity of the end-effector was 0.40 m/s. With the present version of the SpiderBot-II, the maximum linear movement velocity was 0.48 m/s, which was sufficient for feasibility studies of the proposed danger index and the motion control method. All the commanded motions were mainly in x-direction because of the space available for experimentation, as shown in Fig. 7. The free space in y-direction was too small and a reasonable motion span in that direction was not possible. Also, in this work, the reduction in the end-effector velocity and the obstacle avoidance were used as two safety strategies for the cases of VMM and obstacles, respectively.

Similar to refs. [10] and [16], the danger index greater than unity was considered as sever because it was already in per unit system. The threshold δ was taken as 0.2 (i.e. 20%) based on our observations during experiments. However, more experimentation might be needed to determine the threshold and tolerance limits. This is included in our future work when the experiments with elderly would be performed.

Note that the weights (w_d, w_v) were selected tentatively for the feasibility experiments. These weights largely depend on the elderly being assisted by the robot. For our experiments, one choice was to use the weights equal to the variable influence obtained by the subjective set I experiments (Table III), namely $w_v = 0.4$ and $w_d = 0.6$. However, we used both equal to unity to emphasise that both danger components are equally important for user's safety. The proper selection of these weights may require more investigation through experiments with elderly subjects and is part of our future research.

Note that the proposed danger index is based on the motion variables that are easily detectable in operational space. This implies that this index is applicable to all the assistance devices that involve a physical attachment of human and robot and are equivalent to the SpiderBot-II end-effector in operational space (such as RT-walker and KineAssist[33] etc.). Although in this paper we could not present any experimental results with the rehabilitation robots or mobile platform-based assistive robots, we are of the view that our proposed index is also useful for these robots because they are equivalent to the SpiderBot-II end-effector in operational space.

4. Conclusion

This paper introduces a new danger index for estimating the safety of the user interacting with a mobility assistance robot. As mobility assistance task involves physical attachment of robot and human, the previous methods for evaluating the user's safety are not applicable. The proposed index is formulated and validated through extensive experimentation during mobility assistance tasks with subjects in mimicked disability conditions. A motion-control method is introduced that considers the danger index and decides proper safety action on the basis of the proposed danger index. Experimental results are reported in the paper to show the effectiveness of the proposed danger index for enhancing the user' safety in mobility assistance tasks.

Acknowledgments

Authors are grateful to Dr. Yang Won-Ho (Head Rehabilitation Hospital, Cheomdon, Gwangju, South Korea) and Professor Vladimir I. Shin (Gwangju Institute of Science and Technology) for advising on designing the subjective experiment, mimicking the disabilities and statistical analysis. Thanks are also extended to all the participants of subjective experiments.

References

1. OECD Stat Extracts: Country Statistical Profiles, http://stats.oecd.org/wbos/viewhtml.aspx (accessed on Nov. 10, 2007).
2. P. Harmo, T. Taipalus, J. Knuuttila, J. Vallet and A. Halme, "Needs and Solutions – Home Automation and Service Robots for the Elderly and Disabled," *Proceedings of IEEE/RSJ International Conference on Intelligent Robots and Systems*, Edmonton, Canada (2005) pp. 3201–3206.
3. M. Suzuki, K. Masamune, L. J. Ji, T. Dohi and H. Yano, "Development of a robot arm controlled by force sensors as a walking aid for elderly," *Robotica* **16**, 537–542 (1998).
4. J. Heinzmann and A. Zelinsky, "Quantitative safety guarantees for physical human–robot interaction," *Int. J. Robot. Res.* **22**(7–8), 479–504 (2003).
5. A. Bicchi, M. Peshkin and E. Colgate, *Safety for Physical Human-Robot Interaction* (Springer Handbook of Robotics, Springer, Verlag, 2008).
6. B. Graf, M. Hans and R. Schraft, "Care-O-bot II-development of a next generation robotic home assistance," *Auton. Robots* **16**(2), 193–205 (2004).
7. R. Bostelman and J. Albus, "A Multipurpose Robotic Wheelchair and Rehabilitation Device for the Home," *Proceedings of IEEE/RSJ International Conference on Robots and Intelligent Systems*, CA, USA (2007) pp. 3348–3353.
8. C. W. Gadd, "Use of Weighted Impulse Criterion for Estimating Injury Hazard," *Proceedings of 10th Stapp Car Crash Conference*, New York, USA (1966) pp. 164–174.
9. J. Versace, "A Review of Severity Index," *Proceedings of 15th Stapp Car Crash Conference*, New York, USA (1971) pp. 771–796.
10. K. Ikuta, H. Ishii and M. Nokata, "Safety evaluation method of design and control for human-care robots," *Int. J. Robot. Res.* **22**(5), 281–297 (2003).
11. A. Bicchi and G. Tonietti, "Fast and soft-arm tactics," *IEEE Robot. Autom. Mag.* **Jun**, 22–33 (2004).
12. A. DeLuca, A. Albu-Schäffer, S. Haddadin and G. Hirzinger, "Collision Detection and Safe Reaction with the DLR-III

https://doi.org/10.1017/S0263574710000706 Published online by Cambridge University Press

Lightweight Manipulator Arm," *Proceedings of Intelligent Robots and Systems*, Beijing, China (2006) pp. 1623–1630.
13. D. Formica, L. Zollo and E. Guglielmelli, "Torque-Dependent Compliance Control in the Joint Space of an Operational Robotic Machine for Motor Therapy," *Proceedings of 9th IEEE International Conference on Rehabilitation Robotics*, Chicago, IL, USA (2005) pp. 341–344.
14. G. Hirzinger, N. Sporer, A. Albu-Schaffer, A. Hahnle and A. Pascuccu, "DLR's Torque Controlled Light Weight Robot III – Are We Reaching the Technical Limits Now?," *Proceedings of IEEE International Conference on Robotics and Automation*, Washington, DC, USA (2002) pp. 1710–1716.
15. D. Kulic and E. A. Croft, "Safe Planning for Human–Robot Interaction," *J. Robot. Syst.* **22**(7), 383–396 (2005).
16. D. Kulic and E. A. Croft, "Real-time safety for human–robot interaction", *Robot. Auton. Syst.* **54**(1), 1–12 (2006).
17. H. O. Lim and K. Tanie, "Collision-tolerant control of human-friendly robot with viscoelastic trunk," *IEEE/ASME Trans. Mechatronics* **4**(4), 417–427 (1999).
18. H. Liu, X. Deng and H. Zha, "A Planning Method for Safe Interaction Between Human Arms and Robot Manipulators," *Proceedings of IEEE/RSJ International Conference on Intelligent Robots and System*, Canada (2005) pp. 2724–2730.
19. J. Park and O. Khatib, "Multi-link, Multi-contact Force Control for Manipulators," *Proceedings of IEEE International Conference on Robotics and Automation*, Spain (2005) pp. 3624–3629.
20. A. Pervez and J. Ryu "Active Compliance Control Through Danger Estimate for Safe Physical Human Robot Interaction," *Proceedings of International Conference on Advanced Robots*, Korea (2007) pp. 561–566.
21. K. Salisbury, W. Townsend, B. Eberman and D. DiPietro, "Preliminary Design of a Whole-Arm Manipulation System," *Proceedings of IEEE International Conference on Robotics and Automation*, Leuven, Belgium, USA (1988) pp. 254–260.
22. T. Wosch, W. Neubauer, G. V. Wichert and Z. Kemeny. "Robot Motion Control for Assistance Tasks," *Proceedings of 11th IEEE International Workshop on Robot and Human Interactive Communication*, Berlin, Germany (Sep. 25–27, 2002) pp. 524–529.
23. Y. Yamada, Y. Hirasawa, S. Huang, Y. Umetani and K. Suita, "Human–robot contact in the safeguarding space," *IEEE/ASME Trans. Mechatronics* **2**(4), 230–236 (1997).
24. M. Zinn, B. Roth, O. Khatib and J. K. Salisbury, "A new approach for human-friendly robot design," *Int. J. Robot. Res.* **23**(4–5), 379–398 (2004).
25. L. Zollo, L. Dipietro, B. Siciliano, E. Guglielmelli and P. Dario, "A bio-inspired approach for regulating and measuring visco-elastic properties of a robot arm," *J. Robot. Syst.* **22**(8), 397–419 (2005).
26. L. Zollo, B. Siciliano, C. Laschi, G. Teti and P. Dario, "An experimental study on compliance control for a redundant personal robot arm," *Robot. Auton. Syst.* **44**, 101–129 (2003).
27. M. Spenko, H. Yu and S. Dubowsky, "Robotic personal aid for mobility and monitoring for the elderly," *IEEE Trans. Neural Syst. Rehabil. Eng.* **14**(3), 344–351 (2006).
28. O. Chuy Jr., Y. Hirata and K. Kosuge, "A new control approach for a robotic walking support system in adapting user characteristics," *IEEE Trans. Syst., Man Cybern. – Part C: Appl. Rev.* **36**(6), 725–733 (2006).
29. O. Chuy Jr., Y. Hirata, Z. Wang and K. Kosuge, "A control approach based on passive behavior to enhance user interaction," *IEEE Trans. Robot.* **23**(5), 899–908 (2007).
30. Y. Hirata, A. Hara and K. Kosuge, "Motion Control of Passive Walking Support System Based on Environment Information," *Proceedings of IEEE International Conference on Robotics and Automation*, Spain (2005) pp. 2921–2926.
31. G. Lacey and K. M. Dawson-Howe, "The application of robotics to a mobility aid for the elderly blind," *Robot. Auton. Syst.* **23**(4), 245–252 (1998).
32. A. Fattah, S. K. Agrawal, G. Catlin and J. Hamnett, "Design of a passive gravity-balanced assistive device for sit-to-stand tasks," *J. Mech. Des.* **128**, 1122–1129 (2006).
33. M. A. Peshkin, D. A. Brown, J. J. Santose-Munne, A. Makhlin, E. Lewis, J. E. Colgate, J. Patton and D. Schwandt, "KineAssist: A Robotic Overground Base and Balance Training Device," *Proceedings of IEEE 9th International Conference on Rehabilitation Robotics*, Chicago, IL, USA (2005) pp. 241–246.
34. A. Pervez and J. Ryu, "Safe physical human robot interaction – past, present and future," *J. Mech. Sci. Technol.* **22**(3), 469–483 (2008).
35. O. Khatib, "Real Time Obstacle Avoidance for Manipulators and Mobile Robots," *Proceedings of IEEE International Conference on Robotics and Automation*, IEEE, St. Louis, MO, USA (1985), vol. 2, pp. 500–505.
36. J. Ryu, B. Kim, H. S. Farahani and S. Kim, "A new silver robot platform for the elderly and the handicapped: SpiderBot-assistance scenario and concept design," *Int. J. Hum.-Friendly Welfare Robot. Syst.* **5**(3), 9–16 (2004).
37. A. R. Rentscher, R. A. Cooper, V. Blasch and M. Boninger, "Intelligent walkers for the elderly: Performance and safety testing of VA-PAMAID robotic walker," *J. Rehabil. Res. Dev.* **40**(5), 423–432 (2003).
38. S. Dubowsky, F. Genot, S. Godding and H. Kozono, "PAMM-A Robotic Aid to the Elderly for Mobility Assistance and Monitoring: A 'Helping Hand' for the Elderly," *Proceedings of IEEE International Conference on Robotics and Automation*, CA, USA (2000) pp. 570–576.
39. A. Pervez, Y. A. Lim, J. Park and J. Ryu, "SpiderBot-II: Design, Control and Posture Balancing Experimentation," *Proceedings of 1st Korean Intelligent Robot Summer Conference*, Korea (2006) pp. 288–295.
40. H. Yu, M. Spenko and S. Dubowsky, "An adaptive shared control system for an intelligent mobility aid for the elderly," *Auton. Robots* **15**, 53–66 (2003).
41. R. A. Washburn, K. W. Smith, A. M. Jette and C. A. Janney, "The physical activity scale for the elderly (PASE): Development and evaluation," *J. Clin. Epidemiol.* **46**(2), 153–l62 (1993).
42. A. Pervez, Safe and Comfortable Physical Human-Robot Interaction: Evaluation Indices and Control *Ph.D. Thesis* (Deptt. of Mechatronics, Gwangju Institute of Science and Technology Gwangju, Republic of Korea, 2009).
43. Y. Laufer, "The use of walking aids in the rehabilitation of stroke patients," *Rev. Clin. Gerontology* **14**(2), 137–144 (2004).
44. Y. Schutz, S. Weinsier, P. Terrierl and D. Durrerl, "A new accelerometric method to assess the daily walking practice," *Int. J. Obesity* **26**, 111–118 (2002).
45. S. Malki, G. Deepak, V. Mohanna, M. Ringhofer and L. Spaanenburg, "Velocity Measurement by a Vision Sensor," *CIMSA 2006 – IEEE International Conference on Computational Intelligence for Measurement Systems and Applications*, La Coruna, Spain (2006).
46. H. S. Han and J. Kim, "A comparison of screening methods: Selecting important design variables for modeling product usability," *Int. J. Ind. Ergon.* **32**, 189–198 (2003).
47. D. C. Montgomery and G. C. Runger, *Applied Statistics and Probability for Engineers* (John Wiley & Sons, USA, 1994).
48. Y. Motoji, N. Yanai and A. Mohri, "Trajectory control of incompletely restrained parallel wire-suspended mechanism based on inverse dynamics," *IEEE Trans. Robot.* **20**(5), 840–850 (2004).
49. A. Pervez, Y. A. Lim, H. Park and J. Ryu, "A New Physical Interaction Control Strategy for Safe and Comfortable Walking Support System," *Proceedings of 2nd Korean Intelligent Robot Summer Conference,* Kangwon, Korea (2007) pp. 75–82.
50. A. Pervez, Y. A. Lim, H. Park and J. Ryu, "Active Synchronized Motion Control for Comfortable Walking Support," *Proceedings of International Conference on Control, Automation and Systems*, Seoul, Korea (2007) pp. 2714–2718.

https://doi.org/10.1017/S0263574710000706 Published online by Cambridge University Press

Appendix A

A.1. Dynamics of walking assistance

In fact, the nature of physical attachment of human body with the robot during mobility assistance tasks is very complex to model. However, a simplified double mass-damper-spring model may be used to analyze the basic dynamics of walking assistance scenario (such as HLPR Chair[7] shown in Fig. 1(b) or KineAssist[33]), as shown in Fig. A1.

The system of equations for this model is given by

$$m_r\ddot{x}_r + b(\dot{x}_r - \dot{x}_h) + k(x_r - x_h) = u_r, \qquad \text{(A 1)}$$

$$m_h\ddot{x}_h + b(\dot{x}_h - \dot{x}_r) + k(x_h - x_r) = u_h. \qquad \text{(A 2)}$$

Here, subscripts h and r stand for human and robot, respectively. In these equations, first acceleration terms are the components of force that are used to accelerate the masses. The robot–human interaction is represented by terms $b(\dot{x}_r - \dot{x}_h) + k(x_r - x_h)$, with b as the damping (i.e. energy dissipation component) and k as stiffness of human–robot physical attachment. The interaction term can be equivalently represented as

$$b(\dot{x}_r - \dot{x}_h) + k(x_r - x_h) \equiv b(\dot{x}_r - \dot{x}_h) + k\int(\dot{x}_r - \dot{x}_h)dt.$$

Note that $(\dot{x}_r - \dot{x}_h)$ is VMM described throughout the paper. For a very harmonious walking assistance, both bodies move with the same velocity maintaining the same relative displacement between the user and the robot. In this case the interaction force term $b(\dot{x}_r - \dot{x}h) + k(x_r - x_h)$ is not changing. For inharmonious walking assistance, there are sizable mismatches in the relative positions and velocities so that the interaction force changes abruptly. This may destabilise the user by pushing/pulling and thus leading to a falling accident. Therefore, we conclude from this discussion that detecting VMM is very important for user's safety and that VMM can be estimated through interaction force variations.

A.2. Estimation of Velocity-mismatch

Actually, we are interested in the estimation of Δv due to VMM (described in Section 2.2). Note that Δv is a scalar measure of VMM given by Eq. (4). It is positive if assistive robot is pulling/pushing the user to comply with robot velocity, and is negative if retarding the user's self-motion.

From Robot theory, we know that $f_i = J_i^{-T}\boldsymbol{F}$, with $\boldsymbol{f}$ as vector of joint forces, $\boldsymbol{F}$ as wrench applied at an end-effector and $\boldsymbol{J}$ as the Jacobian matrix. We define T_n as the vector of nominal wire tensions measured when there is no VMM between user and robot in walking assistance scenario. We assume that $\boldsymbol{F}$ and $\boldsymbol{F}'$ are the wrenches applied at an end-effector because of body weight, with and without VMM, respectively. We further assume that there is no appreciable wire angle change between two consecutive wire tension measurements, and that the Jacobian matrix is almost same for consecutive measurements,

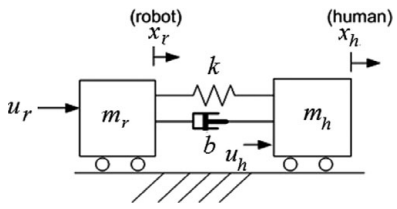


Fig. A1. Equivalent dynamic model of walking assistance.

$$f_i = J_i^{-T}\boldsymbol{F}, \qquad \text{(A 3)}$$

$$f_i' = J_i^{-T}\boldsymbol{F}'. \qquad \text{(A 4)}$$

Thus, using the above assumptions, we have

$$\frac{f_i' - f_i}{f_i} = \frac{\boldsymbol{F}' - \boldsymbol{F}}{\boldsymbol{F}} \Rightarrow \frac{\Delta T_i}{T_i} = \frac{\Delta \boldsymbol{F}}{\boldsymbol{F}}. \qquad \text{(A 5)}$$

The physical meaning of Eq. (A5) is that variation in joint forces, from their respective nominal values, are mainly due to the force generated by VMM. The joint forces are measured in terms of wire tensions (T_i) because wires can only pull in wire direction and cannot apply forces in other directions. Therefore, the variation in joint velocity from its nominal velocity should be proportional to variation in the respective wire tension. Note that the above formulation is true only for positive wire tensions and cannot be applied when any wire is slack.

For SpiderBot-II, the interaction force and consequently the VMM can be estimated through wire-tension variations using a heuristic Eq. (A6)

$$\Delta v = \frac{1}{4}\sum_{i=1}^{4}(K_i sign(\Delta L_i)\Delta T_i), \qquad \text{(A 6)}$$

where K_i is a positive constant ($K_i = 0.0004$, determined experimentally) and ΔT_i is the variation in ith wire tension, from its nominal value T_{iN} that is preset by trial walking (with the help of a therapist).

The rationale of Eq. (A6) is the fact that when there is VMM, the wires pulling and releasing the end-effectors show opposite behaviours. For example, if the speed of user is slower (faster) than that of end-effector, then the tensions in wires 1 and 2 (pulling the end-effector) will increase (decrease), whereas those in wires 3 and 4 (releasing the end-effector) will decrease (increase). By simply adding the variations in wire tensions may cancel each other and hence VMM, Δv, will not be detectable. Thus, Eq. (A6) takes care of this problem and provides a detectable VMM signal.

Appendix B: SpiderBot-II – mechanism and kinematics

SpiderBot-II[42] is an incompletely restrained parallel wire-driven system intended to be used as a service robot for elderly and handicapped persons in the indoor environment. The concept of application scenarios for SpiderBot can be found in ref. [36].

https://doi.org/10.1017/S0263574710000706 Published online by Cambridge University Press

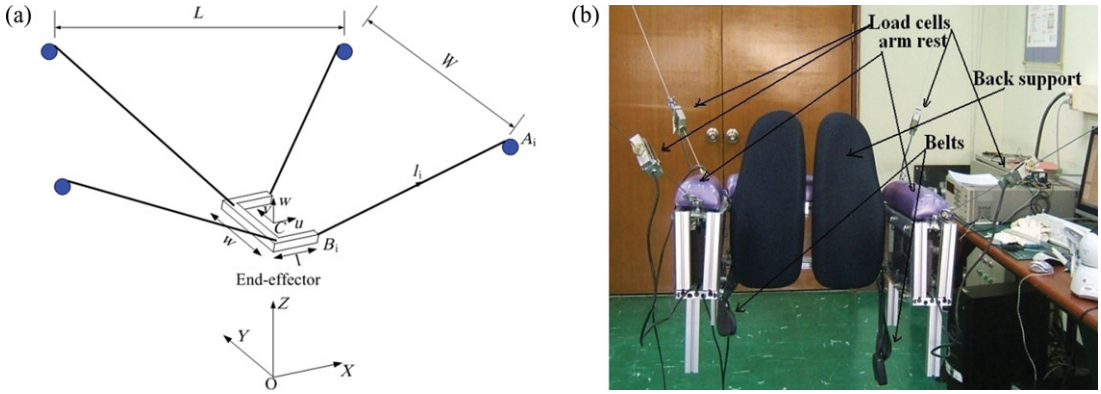


Fig. B1. SpiderBot-II. (a) concept, and (b) end-effector.

B.1. Mechanism overview

Figure B1(a) shows the overall mechanical architecture with one conceptual design of an end-effector for mobility assistance applications. It consists of an end-effector (Fig. B1(b)) suspended by four wires passing through pulleys that are installed at four corners of the room. The wire lengths for a desired pose of the end-effector are computed by an inverse kinematics model and realised by varying the wires' lengths through AC servomotors (HC-KFS-23 from Mitsubishi Inc.). The motors are installed together at one corner of the room and the electrical parts, including servo amplifiers (MR-J2S-20A) for motors and circuit breakers etc., are installed in a control cabinet placed away from the end-effector (and user) due to safety reasons.

The control of SpiderBot-II is achieved through an eight-axis PCI bus-based multi-motion controller (MMC) card and four servo-amplifiers (MR-J2S-20A), one for each motor. Table B1 lists the sensors and actuators used with SpiderBot-II. Currently, four out of eight axes of MMC control card are being used, each axis controlling one AC servomotor. Each servomotor is geared with 25:1 gear ratio and is equipped with a rotary encoder having a resolution of 4000 pulses per revolution. The MMC board implements PID control at low level and can be programmed in Visual C++. The MMC board also allows implementing the user-defined trajectory through a *set_interpolation*() function. We implemented trapezoidal trajectory for each axis controller to achieve a soft start continuous motion control of an end-effector. This avoids the abrupt velocity change that in turn avoids the jerks to the user.

B.2. Inverse kinematics

The inverse kinematics is a calculation problem of wire lengths corresponding to a given pose with zero acceleration and velocities. A global frame A (O-XYZ) was assigned at the centre of the room and a body referenced frame B ($C - uvw$) was assigned at the geometrical centre of the end-effector. It was assumed that the geometrical centre and the centre of gravity coincided. Each wire has a frame (A_{i-xyz}) assigned in such a way that its z-axis is aligned along the wire pointing from A_i to B_i and x-axis is pointing towards the inside of workspace. The y-axis of each frame is assigned according to right hand rule. The orientation of frames at wires with respect to global frame can be described by a rotation of angle ϕ_i about global z_i-axis followed by an angle of θ_i about y_i-axis. The assigned frames and workspace (L, W, H) can be seen in Fig. B1(a), where H is the height of pulleys' installation, L is the length and W is the width of the workspace (room).

The inverse kinematics of an incompletely restrained system is dependent on its dynamics.[48] The dynamic model of SpiderBot-II is given by ref. [49]

$$\boldsymbol{A}\tau = \boldsymbol{B}, \tag{B 1}$$

Table B1. List of parts for SpiderBot-II.

S. No.	Parts	Specifications
1.	Motors	Mitsubishi Electric Inc. HC-KFS23, 3AC 118V, 1.1A, 200 W, 3000 rpm.
2.	Gears	SEJINIGB Inc. ED065-25-A060AE, 25:1.
3.	Encoders	131,072 ppr, Quadrature.
4.	Load cells	SenseTech Inc., SUU-100K, 100 kgf, Instrumentation Amplifier: ST-AMP.
5.	Inertial sensor	Crossbow Inc., DMU-AHRS300CA, $\pm 1^{\circ}$.
6.	Controller card	Samsung Electronics MMCBDPV81PNA, 8 axes, MMC board PCI bus, Full Size, Sample Time 4 m Sec.
7.	Servo Amplifiers	Mitsubishi Electric Inc., MR-J2S-20A: 3-phase, 200 to 300VAC, 50/60 Hz or 1-Phase 230 VAC, 50/60 Hz.

https://doi.org/10.1017/S0263574710000706 Published online by Cambridge University Press

where

$$\boldsymbol{A} = \begin{bmatrix} \frac{l_1}{\overline{CB}_1 \times l_1} & \frac{l_2}{\overline{CB}_2 \times l_2} & \frac{l_3}{\overline{CB}_3 \times l_3} & \frac{l_4}{\overline{CB}_4 \times l_4} \end{bmatrix} = \boldsymbol{J}^T, \tag{B 2}$$

$$\tau = [\, T_1 \; T_2 \; T_3 \; T_4 \,]^T, \tag{B 3}$$

$$\boldsymbol{B} = [m\ddot{X} - \boldsymbol{g} \quad \boldsymbol{I}\dot{\omega} + \boldsymbol{\omega} \times \boldsymbol{I}\omega\,]^T. \tag{B 4}$$

The rank of matrix A is four and only four degrees of freedom can be controlled with the current design of SpiderBot-II. The vector l_i in matrix A is the unit vector along the ith wire and $\overline{CB}_i = {}^A R_B \overline{CB}_i^e$, where ${}^A R_B$ is the rotation matrix of the end-effector platform body in global frame (A) and $\overline{CB}_i^e$ is the position vector of ith wire connection point at end-effector in body reference frame (B). As the wire-extraction points (A_i) in the SpiderBot-II are fixed, so the entries in matrix A will be constant as long as the tensions in the wires are positive. Under positive tension condition,[49] the wire lengths and wire vectors are given by

$$L_i = \|\overline{A_i B_i}\| = \|\overline{A_i O} + \overline{OC} + \overline{CB_i}\|, \tag{B 5}$$

$$l_i = -\frac{\overline{A_i B_i}}{L_i} = [\, l_{ix} \; l_{iy} \; l_{iz} \,]^T, \tag{B 6}$$

where L_i and l_i are the ith wire's length and unit vector, respectively. In Eqs. (B5) and (B6), $\overline{A_i B_i}$ is vector of ith wire length expressed in global frame, A $(O\text{-}XYZ)$, $\overline{OC}$ is the position vector of the end-effector frame B $(C - uvw)$ expressed in global frame A, $\overline{CB}_i = {}^A R_B \overline{CB}_i^e$ with ${}^A R_B = R_{\phi,z} R_{\theta,y} R_{\psi,x}$ as the rotation matrix and $\overline{CB}_i^e$ as the position vector of ith wire connection point at end-effector in body reference frame, B and $\overline{A_i O}$ is the position vector of ith wire-extraction point in frame A. Frames A and B are shown in Fig. B1(a).

B.3. Forward kinematics

The forward kinematics computes the actual pose of end-effector for given wire lengths. As Eq. (B5) (four equations with six unknowns) has multiple solutions for the end-effector pose for given wire lengths, an inertial sensor (Crossbow Inc. AHRS300-100) is used to get the actual orientation, $\Theta = (\, \psi \; \theta \; \phi \,)^T$. The position vector $(\, x \; y \; z \,)^T$ can be computed for the given wire lengths and the end-effector orientation. The end-effector pose is computed as[50]

$$\boldsymbol{X} = \boldsymbol{X}_p + \boldsymbol{J}(\boldsymbol{L} - \boldsymbol{L}_c), \tag{B 7}$$

where $\boldsymbol{X} = [\, x \; y \; z \; \psi \; \theta \; \phi \,]^T$ is the end-effector pose in current iteration, $\boldsymbol{X}_p$ is the end-effector pose during previous iteration, $\boldsymbol{L}$ is the actual (measured) wire lengths vector and L_c is the wire lengths vector computed in current iteration using Eq. (B5) and $\boldsymbol{J}$ is the Jacobian matrix defined in Eq. (B2). The simulation results show that due to the orientation information, less than five iterations ($\approx$0.6ms) are sufficient for convergence.

Appendix C

C.1. Questionnaire for experiment of set I

Test 1. Velocity-mismatch.

1.	A high-velocity robot can be dangerous for your safety.	SD	D	U	A	SA
2.	If agreed to 1, then how much is the risk of falling?	0	1	2	3	4
3.	Due to slow moving robot, you feel to pushing the robot.	SD	D	U	A	SA
4.	If agreed to 3, then how much?	0	1	2	3	4

Test 2. Obstacles-in-the-way.

1.	Due to obstacle in the way, you can be hit and get injured.	SD	D	U	A	SA
2.	How much will be the risk of collision if the obstacle is at a *distance* <0.1 m from you?	0	1	2	3	4
3.	How much will be the risk if obstacle is at a *distance* >1 m	0	1	2	3	4

Test 3. Vibration and jerks.

1.	You can fall due to robot' vibrations.	SD	D	U	A	SA
2.	If agreed to 1, then how much is the risk of falling?	0	1	2	3	4
3.	Due to robot's vibrations you feel a force acting on you body.	SD	D	U	A	SA
4.	If agreed to 3, then how much?	0	1	2	3	4
5.	Jerks at robot end-effector can be a source of falling risk.	SD	D	U	A	SA
6.	If agreed to 5, then how much?	0	1	2	3	4

Test 4. Motion-inaccuracy (error between desired position and actual position of robot).

1.	How much will you feel unsafe with an error of *0.25 m* in the final position during walking assistance?	0	1	2	3	4
2.	How much will you be worried with an error of *0.25 m* in the final position during walking assistance?	0	1	2	3	4
3.	How much will you be physically uncomfortable with an error of *0.25 m* error in the final position?	0	1	2	3	4

Test 5. Load-to-push (for passive robots that require user's force to push them).

1.	A robot requiring human force to move can be dangerous.	SD	D	U	A	SA
2.	If agreed to 1, then how much?	0	1	2	3	4

https://doi.org/10.1017/S0263574710000706 Published online by Cambridge University Press

C.2. Questionnaire for experiment of set II

Test 1. Walking assistance with mimicked disability conditions (leg, knee and weak posture balancing) – VMM case.

1.	During phase 1, how much was the risk of falling?	0	1	2	3	4
2.	During phase 2, how much was the risk of falling?	0	1	2	3	4
3.	During phase 3, how much was the risk of falling?	0	1	2	3	4

Test 2. Walking assistance with mimicked disability conditions (leg, knee and weak posture balancing) – obstacles case.

1.	How much can obstacle at distance <0.1 m be dangerous?	0	1	2	3	4
2.	How much can an obstacle be dangerous when at distance >1 m?	0	1	2	3	4

Test 3. Sit-to-stand assistance (from chair).

1	Did robot pull you?	Yes	No			
2.	Did this pulling disturb your balance?	Yes	No			
3.	If yes to 2, then how much?	0	1	2	3	4

Test 4. Lie-to-sit (from bed).

1.	Did robot pull you?	Yes	No			
2.	Did this pulling disturb your balance?	Yes	No			
3.	If yes to 2, how much?	0	1	2	3	4

Appendix D: Experiments With SpiderBot-II

In order to give a better insight of the experiments that were carried out for validation of the proposed danger index, we briefly describe the experimental results with one of the subjects and discuss only important events. Table D1 provides an overview of the assistance scenarios, disability conditions and cases that were considered for the experiments.

D.1. Walking assistance

D.1.1. Walking assistance with leg disability. (a) Case 1. Velocity-mismatch: Figure D1 shows the experimental results during walking assistance of a subject with mimicked leg disability. In this experiment, the effect of VMM on the danger index was investigated by moving SpiderBot-II on an obstacle-free path. SpiderBot-II started its motion at time $t = 0.5$ s, as can be observed from curve x in Fig. D1(a). The end-effector velocity was varied at $t \approx 5.5$ s and $8\,s$, and thus three phases ((1) $t \approx 0.5 - 5.5$ s, (2) $t \approx 5.5 - 8$ s and (3) $t \approx 8 - 13$ s) were generated. For the subjective data, subjects were asked to rank the level of risk to his/her safety during each phase, which was compared to the average value of the danger index (shown by solid line) in each phase through t-test for correlation (Section 3.6.2). Owing to the mimicked leg disability, subject was unable to walk with the same velocity as that of end-effector, which can be observed by wire tension curves in Fig. D1(b). It can be seen in Fig. D1(a) that average VMM (shown by black solid line on the VMM curve) in phase 2 was larger than those in phases 1 and 3. This effect was also reflected in the danger index (D), as shown in Fig. D1(a) because all the other factors were retained to their initial values during the test. Note that distance-to-obstacle was larger than 2 m during the test and thus did not contribute to the danger index.

(b) Case 2. Obstacle case: Figure D2 shows the results for walking assistance experiment with a subject in the mimicked leg disability using SpiderBot-II. In this test, the end-effector velocity was kept constant (curve x in Fig. D2(a)); however, an obstacle was placed at position (1.5, −0.35, 0). The uneven walking due to the mimicked leg disability can be observed by wire tension curves (Fig. D2(b)). Note that in this case, the VMM was very small (∼0.05 m/s) as compared to that of VMM case (∼0.15 m/s) shown in Fig. D1(a). The danger index (D) shown in Fig. D2(a) is due to obstacle coming closer, as evident from $D2O$ curve in Fig. D2(a)). For the subjective data, we divided this test into two phases: in phase 1, the obstacle was far from subject ($D2O > 1$ m), whereas in phase 2, it was close to the subject ($D2O < 0.1$ m). Subjects were asked to rank the level of risk to their safety in each phase that was used to compare with the computed value of danger index through t-test for correlation (Section 3.6.2).

D.1.2. Walking assistance with Knee disability. (a) Case 1. Velocity-mismatch case: Figure D3 shows the experimental results for walking assistance with the mimicked knee disability using SpiderBot-II. Same trajectory was used for this test as that for leg disability case shown in Fig. D1.

Three phases can be observed at ((1) $t \approx 0.5 - 5.5$ s, (2) $t \approx 5.5 - 8$ s and (3) $t \approx 8 - 13$ s) by slope of curve

Table D1. Overview of the assistance scenarios and cases for experiments.

No.	Assistance scenario	Disability condition	Case
1.	Walking	Leg disability	Velocity-mismatch Obstacle
		Knee disability	Velocity-mismatch Obstacle
		Weak posture balancing	Velocity-mismatch Obstacle
2.	Sit-to-stand	Weak posture balancing	Velocity-mismatch
3.	Lie-to-sit	Weak posture balancing	Velocity-mismatch

https://doi.org/10.1017/S0263574710000706 Published online by Cambridge University Press

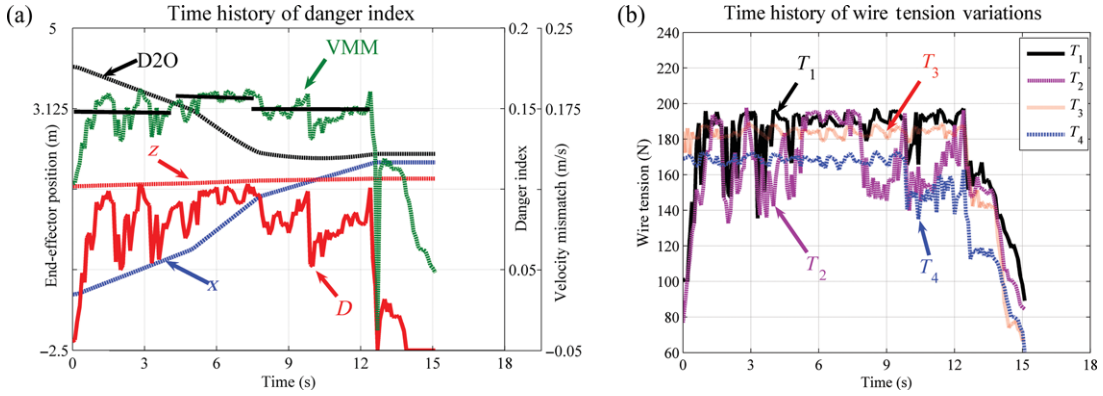


Fig. D1. Walking assistance with leg disability – velocity-mismatch case.

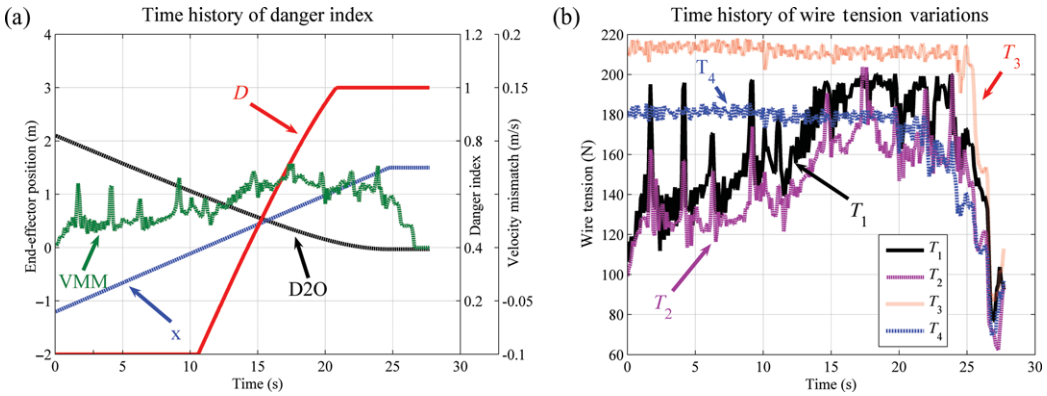


Fig. D2. Walking assistance with leg disability – obstacle case.

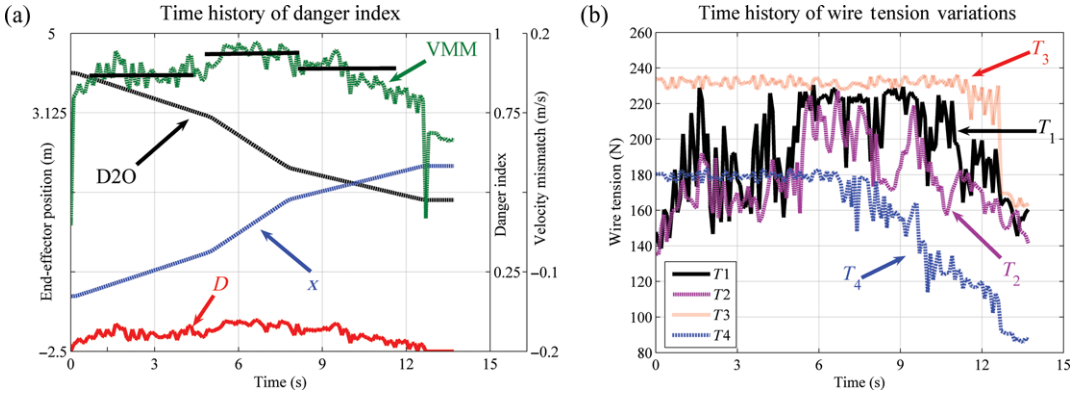


Fig. D3. Walking assistance with knee disability – velocity-mismatch case.

x (Fig. D3(a)). The VMM during phase 2 is the highest and likewise the danger is also larger in this phase (Fig. D3(a)). Similar procedure was adopted to get the subjective and objective data as that for the experiment of VMM case in the mimicked leg disability (Section D.1, case 1).

(b) Case 2. Obstacle case: Figure D4 shows the experimental results for walking assistance experiment with the mimicked knee disability considering an obstacle in the way. Similar to the obstacle case of leg disability, robot velocity was kept constant, as can be seen from the slope of curve x in Fig. D4(a). Oscillations were observed in wire tensions (Fig. D4(b)) because of uneven walking caused by the mimicked knee disability.

The danger index is shown in Fig. D4(a) and it can be observed that the danger index (D) was zero till time $t \approx 8$ s because the VMM was not significant due to constant velocity operation. After $t \approx 8$, D increased rapidly and became unity at $t \approx 16$ s because the end-effector had reached the danger zone, (with ($D2O$ $<$ 0.1 m). Similar procedure was followed to get and compare the subjective and objective data as that for the mimicked leg disability obstacle case (Section D.1, case 2).

D.1.3. Walking assistance with weak posture balancing. (a) Case 1. Velocity-mismatch case: Figure D5 shows the experimental results for walking assistance of a subject with the mimicked weak posture balancing. For such a condition, the subject needs assistance during walking to avoid a falling accident. The three phases of velocity can be identified by slope of curve x in Fig. D5(a). The VMM signal in Fig. D5(a)

https://doi.org/10.1017/S0263574710000706 Published online by Cambridge University Press

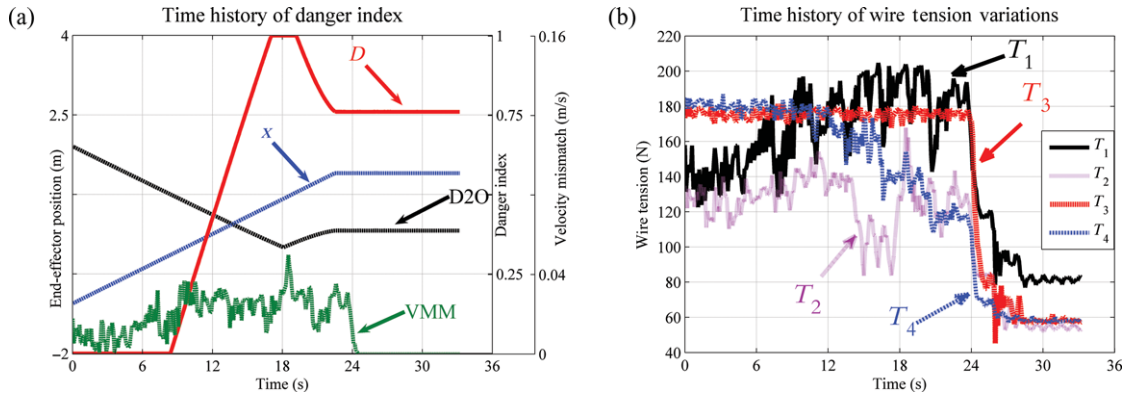


Fig. D4. Walking assistance with knee disability – obstacle case.

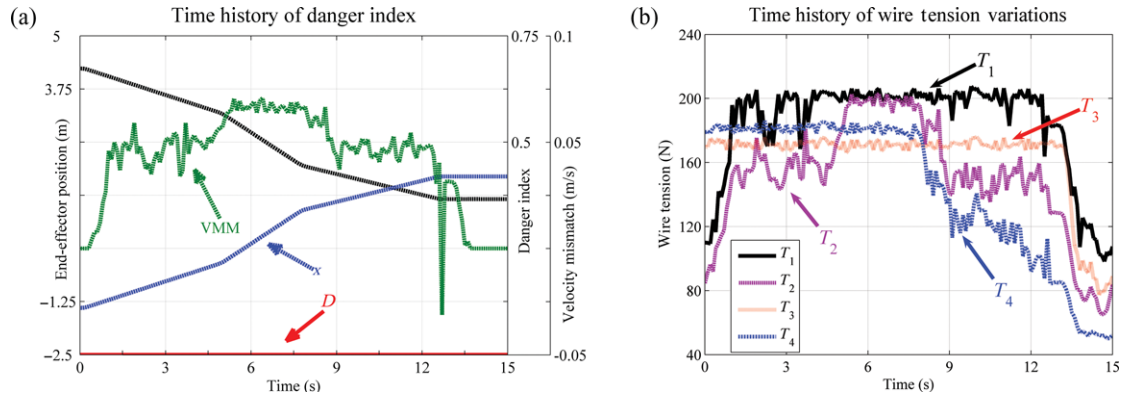


Fig. D5. Walking assistance with weak posture balancing – velocity-mismatch case.

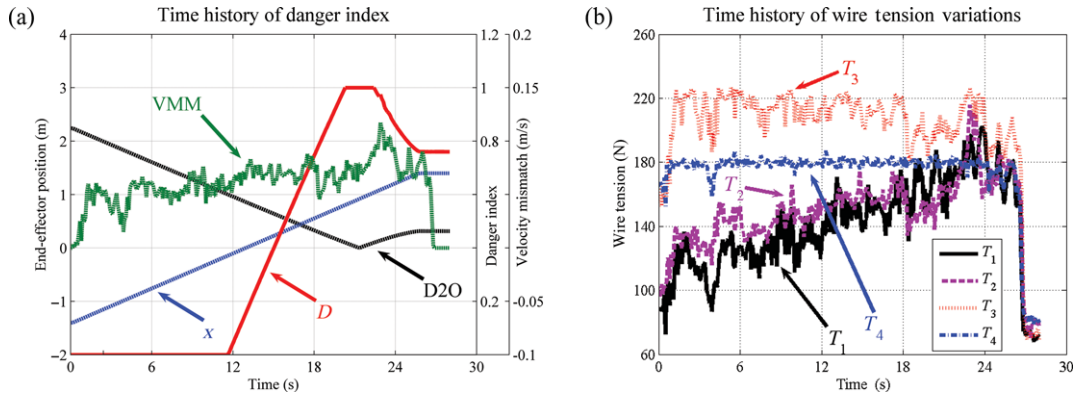


Fig. D6. Walking assistance with weak posture balancing – obstacle case.

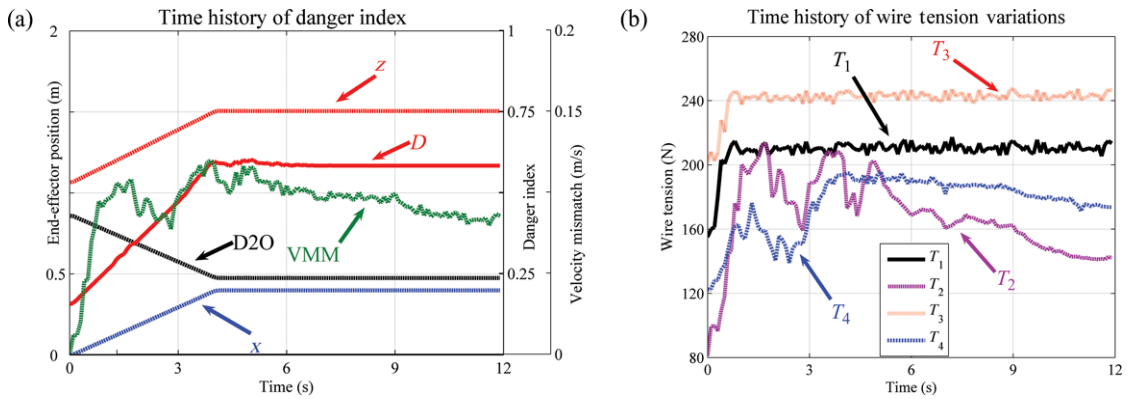


Fig. D7. Sit-to-stand assistance with weak posture balancing using SpiderBot-II.

https://doi.org/10.1017/S0263574710000706 Published online by Cambridge University Press

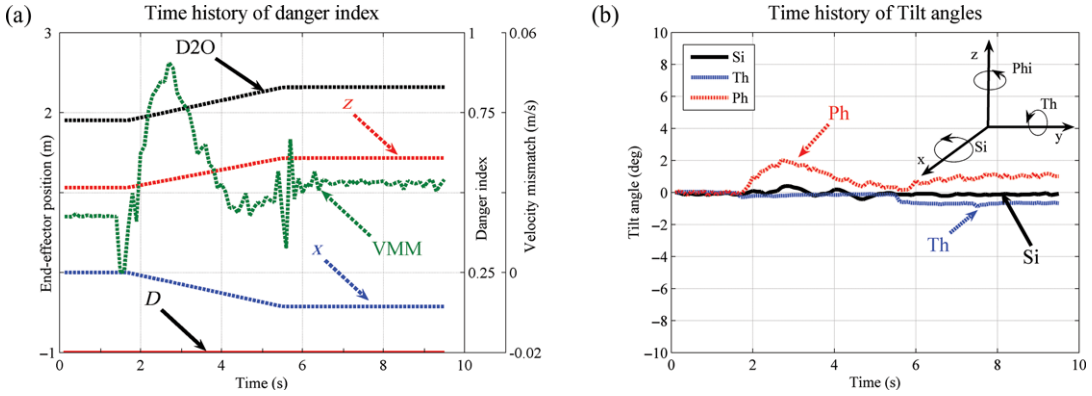


Fig. D8. Lie-to-sit assistance using SpiderBot-II.

shows that VMM in phase 2 ($t \approx 5-8$ s) is higher than that in phases 1 ($t \approx 5-8$ s) and 3 ($t \approx 5-8$ s). However, because the VMM was less than the lower limit of VMM, ΔV_m (0.1 m/s), the danger index (D) was zero implying that leg and knee disabilities are severer than the WP. The procedure for getting and comparing the subjective and objective data was same as described in reference to the case 1 of the mimicked leg disability (Section D.1, case 1).

(b) Case 2. Obstacle case: Figure D6 shows the experimental results with the mimicked weak posture balancing considering an obstacle in the way. The motion was started at time $t \approx 0$ s and completed at $t \approx 25$ s (Fig. D6(a)). The oscillations in angle about x-axis (si) are due to non-smooth walking of the subject. The danger index is mainly due to obstacle because the VMM is less than the lower limit (0.1 m/s). Similar procedure was adopted to acquire the subjective and objective data for t-test as that for obstacle case in the mimicked leg disability experiment described in Section D.1.

D.2. Sit-to-stand assistance with weak posture balancing

Figure D7 shows the experimental results for sit-to-stand assistance of a subject with the mimicked weak posture-balancing capability. In this test, subject was initially sitting on a chair and could not stand up due to WP. The trajectory for SpiderBot-II consisted of motion in forward (x-axis) as well as upward directions (z-axis), as shown by curves x and z in Fig. D7(a). The subject needed the remaining force to be supplied during the rising phase. The force supplied by the robot can be viewed by wire tension curves in Fig. D7(b). The maximum force was needed at time $t \approx 1.5$s, when the subject left the seat. The force was reduced at $t \approx 3$s, when the subject gained the momentum to stand up. The VMM shows the same behaviour as followed by the remaining force required by the subject. Accordingly, the danger index (D) also increased in the transition period but remained constant afterwards due to obstacle, as can be seen by the $D2O$ curve in Fig. D7(a). Subjects were asked to rank the severity of danger to their safety through questionnaire (Appendix C.2). The subjective data were compared through t-test for correlation with the average value of danger index (D) during the test.

D.3. Lie-to-sit assistance with weak posture balancing

Figure D8 shows the results for lie-to-sit assistance experiment performed in the same environment as that shown in Fig. 7. In this case, the robot was moved in forward–upward plane (x–z), as shown in Fig. D8(a). The motion started at time $t \approx 2$ s and ended at $t \approx 5.5$ s. The VMM (<0.05 m/s) was less than the lower limit, ΔV_m (0.1 m/s) and consequently the danger index was also zero during this experiment. Similar procedure was followed to get and compare the subjective and objective data as that for sit-to-stand assistance experiment described in Section D.2.

https://doi.org/10.1017/S0263574710000706 Published online by Cambridge University Press